REPORT DOCUMENTATION PAGE

Form Approved
OMB No. 0704-0188

Public reporting burden for this collection of information is estimated to average 1 hour per response, including the time for reviewing instructions, searching existing data sources, gathering and maintaining the data needed, and completing and reviewing this collection of information. Send comments regarding this burden estimate or any other aspect of this collection of information, including suggestions for reducing this burden to Department of Defense, Washington Headquarters Services, Directorate for Information Operations and Reports (0704-0188), 1215 Jefferson Davis Highway, Suite 1204, Arlington, VA 22202-4302. Respondents should be aware that notwithstanding any other provision of law, no person shall be subject to any penalty for failing to comply with a collection of information if it does not display a currently valid OMB control number. **PLEASE DO NOT RETURN YOUR FORM TO THE ABOVE ADDRESS.**

1. REPORT DATE *(DD-MM-YYYY)*	2. REPORT TYPE	3. DATES COVERED *(From - To)*
06-12-2005	Journal Article	

4. TITLE AND SUBTITLE

The Moment Analysis Method as Applied to the $^2S \rightarrow ^2P$ Transition in Cryogenic Alkali Metal/Rare Gas Matrices (POSTPRINT)

5a. CONTRACT NUMBER

5b. GRANT NUMBER

5c. PROGRAM ELEMENT NUMBER

6. AUTHOR(S)
Heidi A. Terrill Vosbein (Stennis Space Center); Jerry Boatz (AFRL/PRSP);
John W. Kenney (Concordia University)

5d. PROJECT NUMBER
23030423

5e. TASK NUMBER

5f. WORK UNIT NUMBER

7. PERFORMING ORGANIZATION NAME(S) AND ADDRESS(ES)

Air Force Research Laboratory (AFMC)
AFRL/PRSP
10 E. Saturn Blvd.
Edwards AFB CA 93524-7680

8. PERFORMING ORGANIZATION REPORT NUMBER

AFRL-PR-ED-JA-2005-482

9. SPONSORING / MONITORING AGENCY NAME(S) AND ADDRESS(ES)

Air Force Research Laboratory (AFMC)
AFRL/PRS
5 Pollux Drive
Edwards AFB CA 93524-7048

10. SPONSOR/MONITOR'S ACRONYM(S)

11. SPONSOR/MONITOR'S NUMBER(S)
AFRL-PR-ED-JA-2005-482

12. DISTRIBUTION / AVAILABILITY STATEMENT

Approved for public release; distribution unlimited (AFRL-ERS-PAS-05-305)

13. SUPPLEMENTARY NOTES
As published in the Journal of Physical Chemistry, 109 (2005) 11453-11461.

14. ABSTRACT

The moment analysis method (MA) has been tested for the case of $^2S \rightarrow ^2P$ ([core]ns1→[core]np^1) transitions of alkali metal atoms (M) doped into cryogenic rare gas (Rg) matrices using theoretically validated simulations. Theoretical/computational M/Rg system models are constructed with precisely defined parameters that closely mimic known M/Rg systems. Monte Carlo (MC) techniques are then employed to generate simulated absorption and magnetic circular dichroism (MCD) spectra of the $^2S \rightarrow ^2P$ M/Rg transition to which the MA method can be applied with the goal of seeing how effective the MA method is in re-extracting the M/Rg system parameters from these known simulated systems. The MA method is summarized in general, and an assessment is made of the use of MA method in the rigid shift approximation typically used to evaluate M/Rg systems. The MC-MCD simulation technique is summarized and validating evidence is presented. The simulation results and the assumptions used in applying MA to M/Rg systems are evaluated. The simulation results on Na/Ar demonstrate that the MA method does successfully re-extract the ^2P spin-orbit coupling constant and Landé g-factor values initially used to build the simulations. However, assigning physical significance to the cubic and non-cubic Jahn-Teller (JT) vibrational mode parameters in cryogenic M/Rg systems is not supported.

15. SUBJECT TERMS

16. SECURITY CLASSIFICATION OF:			17. LIMITATION OF ABSTRACT	18. NUMBER OF PAGES	19a. NAME OF RESPONSIBLE PERSON
					Dr. Scott A. Shackelford
a. REPORT	b. ABSTRACT	c. THIS PAGE			19b. TELEPHONE NUMBER *(include area code)*
Unclassified	**Unclassified**	**Unclassified**	SAR	10	N/A

Moment Analysis Method As Applied to the $^2S \rightarrow {}^2P$ Transition in Cryogenic Alkali Metal/Rare Gas Matrices†

Heidi A. Terrill Vosbein*

Naval Research Laboratory, Code 7180, Stennis Space Center, Mississippi 39529

Jerry A. Boatz

Air Force Research Laboratory, Space and Missile Propulsion Division, AFRL/PRSP, Edwards AFB, California 93524-7680

John W. Kenney, III

Chemical Physics Laboratory, Concordia University, 1530 Concordia West, Irvine, California 92612

Received: June 30, 2005; In Final Form: October 7, 2005

The moment analysis method (MA) has been tested for the case of $^2S \rightarrow {}^2P$ ([core]$ns^1 \rightarrow$ [core]np^1) transitions of alkali metal atoms (M) doped into cryogenic rare gas (Rg) matrices using theoretically validated simulations. Theoretical/computational M/Rg system models are constructed with precisely defined parameters that closely mimic known M/Rg systems. Monte Carlo (MC) techniques are then employed to generate simulated absorption and magnetic circular dichroism (MCD) spectra of the $^2S \rightarrow {}^2P$ M/Rg transition to which the MA method can be applied with the goal of seeing how effective the MA method is in re-extracting the M/Rg system parameters from these known simulated systems. The MA method is summarized in general, and an assessment is made of the use of the MA method in the rigid shift approximation typically used to evaluate M/Rg systems. The MC-MCD simulation technique is summarized, and validating evidence is presented. The simulation results and the assumptions used in applying MA to M/Rg systems are evaluated. The simulation results on Na/Ar demonstrate that the MA method does successfully re-extract the ^2P spin−orbit coupling constant and Landé *g*-factor values initially used to build the simulations. However, assigning physical significance to the cubic and noncubic Jahn−Teller (JT) vibrational mode parameters in cryogenic M/Rg systems is not supported.

1. Introduction

This study is motivated primarily by a desire to understand and resolve the contradictory interpretations of MCD spectra obtained by using the moment analysis method on similar systems of metal atoms embedded in rare gas matrices.[1−3] For example, the work by Lund et al.[1] assigned a spin−orbit (SO) splitting of -24.5 cm^{-1} for the ^2P term of lithium (Li) in solid argon (Li/Ar), -105 cm^{-1} for Li in solid krypton (Kr), and -220 cm^{-1} for the ^2P term of Li in solid xenon (Xe). Rose,[2,4] working in the same laboratory, reported a ^2P SO splitting of -327 cm^{-1} for Na/Xe and -295 cm^{-1} for Li/Xe. However, another paper[3] had contradictory results, also derived from a moment analysis, reporting SO splitting of 10 cm^{-1} for the ^2P term of Na/Xe. Therefore, a systematic investigation into the moment analysis method as applied to alkali metal/rare gas matrices (M/Rg) systems is in order.

The aforementioned papers use the method of moments or moment analysis to extract physical parameters from the data. These are then used to develop models or theories of the processes producing the values. If the extracted parameters are incorrect, then so too is any interpretation of the data based on those parameters. The moment analysis was used in the M/Rg systems by analogy to f-centers without independent confirmation of its applicability. This was not necessarily an appropriate analogy. An f-center is formed when a negative ion is replaced by an electron in a crystal lattice; substantial interaction between the electron and the surrounding lattice is expected. However, the M/Rg system consists of neutral atoms in a hole in a neutral lattice; it is not so clear that a substantial interaction, as suggested by the experimental, moment analysis derived, SO values, is justified. Therefore, the method should be independently verified for the system in question.

It was found that the theoretically verified absorption/MCD Monte Carlo model[5] produced the same basic absorption and MCD patterns observed experimentally for both spin−orbit splittings in the range reported by the experimentalists for the Na/Rg systems and using the Na free atom SO splitting. Therefore, it was postulated that the moment analysis method as defined for the M/Rg systems was biased to produce large negative spin−orbit values. A computer program was written to do the full moment analysis evaluation of the simulated spectra as well as tabulated experimental spectra. The program was tested on the published experimental spectra to verify that it produced the same values, within tabulation errors, as those published for the various parameters. Once the program was verified in this way, it was applied to the simulated spectra. We expected that both the simulated spectra produced using large negative SO coupling and the simulated spectra using small positive (free-atom value) SO coupling would have large negative moment analysis calculated results for the spin−orbit coupling, because they had the same basic pattern. It was a

† Part of the special issue "Jack Simons Festchrift".

* Corresponding author.

10.1021/jp053592m CCC: $30.25 © 2005 American Chemical Society
Published on Web 12/15/2005

surprise when the MA correctly identified the input SO coupling of each simulation.

2. Overview of the Method of Moments

The method of moments, or moment analysis (MA), provides a consistent way to extract system parameters from spectra. Moment analysis is based on the calculation of band moment integrals over the spectral features, the ratios of which are related to physical quantities. There are two types of moment integrals, initial and central. The forms of the integrals are

$$S_n = \int \nu^n f(\nu)\, \mathrm{d}\nu \tag{2.1}$$

for the initial moments and

$$\overline{S_n} = \int (\nu - \bar{\nu})^n f(\nu)\, \mathrm{d}\nu \tag{2.2}$$

for the central moments where ν in eqs 2.1 and 2.2 is the photon frequency, $f(\nu)$ is the spectral band shape function, n is the order of the moment, and $\bar{\nu}$ is the absorption barycenter. The method of moments can be applied to any distribution function containing a maximum and defined from $-\infty$ to $+\infty$.[6] As a consequence of this, only discrete bands may be considered using this method because the integration must take place between points where the band shape function goes to zero.[7] In practice, this often means that a threshold or background band shape is defined and subtracted from the spectra, making it satisfy this requirement. MA allows different laboratories and research groups to compare results, even if the actual spectra appear quite different due to equipment and/or processing differences.

In the case of IR (infrared) spectra, the spectrum is broken down into sets of Gaussian bands, with integration over each band.[6,8] For electronic absorption and magnetic circular dichroism (MCD) spectra, the integration is over the entire band, with the ratios of moments of various orders from the MCD and absorption compared. An analysis similar to the IR case may be possible if only the electronic absorption spectrum is available.

Hereafter all references to moment analysis (MA) refer to the rigid shift moment analysis (RSMA) method. This technique is widely used in extracting physical parameters, most notably spin−orbit coupling, from the MCD and absorption spectra of atomic and molecular systems. The method was first applied to f-centers[9] but has since been applied to many diverse systems, including the $^2S \rightarrow {}^2P$ absorption and MCD spectra of alkali metals isolated in cryogenic rare gas solids (M/Rg). As can be seen from the moment equations, higher order moments are increasingly less accurate due to the influence of the wings of the band.[7] The n th absorption and MCD moment integrals are[1]

$$A_n = \int \left(\frac{A}{\epsilon}\right)(\epsilon - \bar{\epsilon})^n\, \mathrm{d}\epsilon \tag{2.3}$$

$$M_n = \int \left(\frac{\Delta A'}{\epsilon}\right)(\epsilon - \bar{\epsilon})^n\, \mathrm{d}\epsilon \tag{2.4}$$

where the subscript, n, indicates the order of the moment, $A(\epsilon)$ is the absorption intensity, $\Delta A'(\epsilon)$ is the differential absorption of left vs right circularly polarized light, defined by

$$\Delta A'(\epsilon) = A'_{\mathrm{LCP}}(\epsilon) - A'_{\mathrm{RCP}}(\epsilon) \tag{2.5}$$

TABLE 1: Definitions of MCD Terms

Term	Source	Characteristic Shape
$\mathcal{A}$	Ground or excited state degenerate	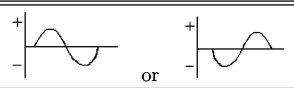
$\mathcal{B}$	Magnetic mixing of zero field energy levels	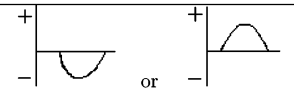
$\mathcal{C}$	Ground state degenerate	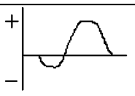

where ϵ is the photon energy and $\bar{\epsilon}$ is the energy of the absorption barycenter.

$$\bar{\epsilon} = \frac{\int A\, \mathrm{d}\epsilon}{\int \left(\frac{A}{\epsilon}\right) \mathrm{d}\epsilon} \tag{2.6}$$

The primed terms indicate that the spectra are measured in the presence of a magnetic field. These equations are of the central moment type, with $f(\nu) = (A/\epsilon)$ and $f(\nu) = (\Delta A'/\epsilon)$ for the absorption and MCD spectra, respectively. For central moments such as these, all odd moments of completely symmetric spectra are zero. Antisymmetric MCD spectra have zero even moments.

The RSMA operates on the assumption that the Born−Oppenheimer (BO) approximation is obeyed in both the ground and excited states and the Franck−Condon (FC) approximation is sufficient for the electronic operator matrix elements. For such systems, the zeroth and first MCD moments, M_0 and M_1, contain all information available from the MCD. In systems where the Jahn−Teller effect (JTE) is in operation, the BO approximation breaks down and higher moments must be used.[10]

MCD spectra are characterized by $\mathcal{A}$, $\mathcal{B}$, and $\mathcal{C}$, terms.[7] In the course of studying systems in which the MCD $\mathcal{B}$ term (see Table 1 for definition of MCD terms) is dominant, Zgierski found that the RSM equations generally used to separate the $\mathcal{A}$ and $\mathcal{B}$ term contributions of the MCD spectra are inaccurate when vibronic effects are present. The RSMA can be used with a vibronically active system[7,10] but it operates on the assumption that the individual electronic transition moments between pairs of states are vibrational coordinate independent and can be described by a Franck−Condon progression. Zgierski points out that this is not a reasonable assumption because "in general, the adiabatic potentials associated with different states are not parallel since electronic excitation changes vibronic force fields. This implies that the energy separation of two coupled states is not a constant but a function of the vibrational coordinates (p 2171)".[11] The magnetic mixing of vibrations can cause the MCD $\mathcal{B}$ term to change sign within the region of a single, isolated allowed electronic transition. Furthermore, the first moment of the MCD spectrum is generally calculated with respect to the center of gravity of the corresponding absorption spectrum and corresponds to the electronic $\mathcal{A}$ term. However, when vibrations are present it often is not equal to the $\mathcal{A}$ term "since the conventional definition of the center of gravity loses its applicability (p 548)".[12] In some cases, the magnetic mixing of vibronic states can simulate the presence of an $\mathcal{A}$ term or vibronic coupling when only a $\mathcal{B}$ term is actually present.[12]

Although the $^2S \rightarrow {}^2P$ transition of interest in the case of the M/Rg systems contains primarily the MCD $\mathcal{A}$ and $\mathcal{C}$ terms, consideration of the effects of vibrations and the magnetic field on the spectra is very important. It is possible that matrix effects also contribute to the mixing of the zero-field states, making the MCD $\mathcal{B}$ term and vibronic coordinates more important.

Zgierski labels all deviations from the standard FC progression "non-Condon" effects. He asserts that all MCD spectra are non-Condon in the sense that the overall transition moment will be coordinate dependent if the transition is induced by a perturbation that causes mixing with a third state. Zgierski lists several references in which he maintains it has been shown that non-Condon effects are important in vibronically and SO induced absorption-emission spectra, radiationless transitions, and photoelectric spectra.[11]

The MA method is generally applied to experimental systems under the implicit assumption that MA is a valid way to extract system properties. This study constitutes the first simulation test/confirmation of the MA method for extracting the spin−orbit (SO) coupling of M/Rg systems [specifically sodium (Na)/argon (Ar)]. The idea is to build a computer simulated M/Rg system with known SO, vibronic, site symmetry, and thermal parameters and known M−Rg and Rg−Rg interaction potentials and then generate simulated $^2S \rightarrow {}^2P$ electronic absorption and MCD spectra of this simulated M/Rg system. These simulated spectra are then subjected to a full MA treatment, and the SO, vibronic, symmetry, and thermal parameters thus extracted are compared to the original parameters as an independent check of the viability of the MA method. Only one other computer study of a moment analysis method is known to the authors. It considers the effects of spectral asymmetries on the higher order moments.[6,8] The first of these papers describes the spectral band distortions associated with the detection equipment in IR measurements and a technique for using band moments to extract information. The second explores ways in which asymmetries affect the higher order moments.

3. Specifics of MA for M/Rg Systems

In the context of this research the MA method has been applied to the absorption and MCD spectra of metals trapped in cryogenic rare gas solids [alkali metal/rare gas;[1−4,13,14] alkaline earth/rare gas;[15,16] transition metal/rare gas[17−25]]. Those of primary interest in high energy density matter (HEDM) research are the alkali metals, Li and Na. As yet there has been very little experimental data on these metals in the lighter rare gases. The Schatz group has obtained absorption and MCD spectra of Li in Ar, Kr, and Xe[1] and Na in Xe.[2,4] Fajardo et al. have shown that alkali metals can exist in multiple trapping sites in Rg matrices including some novel tight trapping sites produced by the laser ablation method.[26−29] Kenney and Stowe have measured MCD spectra of Li/Ar tight trapping sites prepared by laser ablation of Li.[30,31]

After some manipulation, the results of the different absorption and MCD moments can be reduced to four equations relating the zeroth and second absorption moments, and the first, second, and third MCD moments to the physical parameters. They are[1]

$$\frac{M_1}{A_0} = 0.934\left(g - \frac{\zeta}{2kT}\right) \tag{3.1}$$

$$\frac{M_3}{M_1} = \frac{3}{4}\zeta^2 + 3\Delta_C{}^2 + \frac{3}{2}\Delta_{NC}{}^2 \tag{3.2}$$

$$\frac{A_2}{A_0} = \frac{1}{2}\zeta^2 + \Delta_C{}^2 + \Delta_{NC}{}^2 \tag{3.3}$$

$$\frac{M_2}{A_0} = 0.934\frac{\zeta^2}{4kT} \tag{3.4}$$

where ζ is the spin−orbit parameter ($\zeta = {}^2/_3\xi$, ξ is the SO splitting of the ^2P term), Δ_C is the cubic mode parameter, Δ_{NC} is the noncubic mode parameter, g is the Landé g-factor, and k is the Boltzmann constant. Δ_C and Δ_{NC} are used to estimate the relative strengths of the cubic and noncubic Jahn−Teller (JT) vibronic modes in the system. These equations were originally derived for f-centers, therefore the inclusion of trapping site specific/JT vibronic parameters.

In practice, the spin−orbit parameter, ζ, is the slope of the line obtained by plotting M_1/A_0 vs $-0.934/2kT$. The Landé g-factor is calculated from eq 3.1 using this ζ. The squared value of ζ obtained from the slope of eq 3.1 can then be compared to that calculated from the slope obtained by plotting M_2/A_0 vs $0.934/4kT$ (eq 3.4), providing an independent check of the accuracy of the higher order MCD moments.

For the Li/Rg and Na/Xe $^2S \rightarrow {}^2P$ experimental spectra[1,2,4] that have been explored using the MA, the values derived from the MA equations for the ^2P spin−orbit splitting were large and negative. The magnitude of the SO splittings obtained from MA for Li/Ar and Li/Kr are substantially reduced compared with that of Li/Xe.[1] In the Li/Ar spectra, the calculated SO splitting is only a little more than 10% of the Li/Xe value, and the SO splitting in Li/Kr is approximately half the MA derived value for Li/Xe. These large negative values—several orders of magnitude larger and of opposite sign than the free atom values—seemed unphysical. The explanation of these results was that there was substantial interaction between the metal atom valence electron and the rare gas. Although such delocalization of the electron seems reasonable for the f-center, where an electron is trapped in a negative ion vacancy, it seems less likely for the case of a metal atom in a rare gas. Furthermore, simulations on the effects of varying the SO splitting of the impurity atom have shown that the same gross spectral features could be obtained using either large negative spin−orbit splitting or small positive spin−orbit splitting. Examination of eq 3.1 shows that for M_1/A_0 greater than zero, ζ is restricted to either a very small positive or negative value. The experimental M/Rg spectra from the literature generally have roughly symmetric absorption, with the exception of M/xenon, and MCD spectra characterized by either two down peaks (negative) and one up peak or one down peak and two up peaks with increasing energy. Consequently, A_0 and M_1 will both have positive signs. This tends to predispose the results to require negative SO splitting. Also, the "best fit" to the data described in the literature[4] seemed rather arbitrary.

The observed spectra and MA results have been attributed[1,2,4] to the combination of strong SO coupling and strong dynamic Jahn−Teller effect (DJTE) in the ^2P manifold. The JTE is the lifting of electronic degeneracies of atoms or molecules in symmetric trapping sites as the trapping site is distorted by point-group specific vibrations. The DJTE occurs when the trapping site dynamically accesses one or more of the Jahn−Teller (JT) active vibrations. Although the seemingly-too-large-magnitude, negative SO coupling results have been supported by this simulation test of the moment analysis method and a simplified first principles calculation,[32] the physical explanations of their source are lacking. The combination of strong SO coupling and strong DJTE are contradicted by research by Ham.[33] In the absence of strong vibrations, SO coupling can be established and a stable equilibrium balancing the effects of the neighboring Rg atoms against the orbit of the valence M electron may be reached. When the JTE, or any vibration, is present in the solid, it becomes much more difficult to establish an equilibrium between the two. Ham described the result of this disruption of

the orbit of the electron as "quenching" the orbital angular momentum.[33] The quenching of the orbital angular momentum results in a reduction in the magnitude of the SO coupling. The experimental M/Rg MA results indicate an *increase* in the magnitude of the SO coupling, although the sign has changed. If the SO coupling is strong enough, it can stabilize the atom against the JTE, though the magnitude of the SO coupling may still be reduced.[33] The basic conclusion that may be drawn from this is that it is not possible to have both strong SO coupling and a strong JT interaction. Furthermore, the JTE is defined as the vibronic lifting of electronic degeneracies of atoms or molecules in *symmetric* sites. It is unlikely that all M/Rg trapping sites can be defined as symmetric.

Another theory proposed to explain the M/Rg MA results invoked the external heavy atom effect (EHAE) as well as requiring symmetric JT splitting of the M $J = {}^3/_2$ energy level and a 12-nearest-neighbor supermolecule.[34] This theory has several problems. First of all, the EHAE simply does not apply to the M/Rg systems. Although one manifestation of the effect can produce a "strong increase of the effective spin−orbit coupling,[35]" it tends to be restricted to the case of $\Delta J = 0$, and $J \neq 0$, a situation that is not possible between rare gases having integer J and alkali metals having half-integer J. Furthermore, the rare gases neon and argon are not heavy atoms, yet the M/Ar spectra are very similar to those of M/Kr and M/Xe systems. Na/Ne absorption spectra do not exhibit the triplet structure seen in other M/Rg combinations; however, it could be that the structure is simply not resolved.[27] MCD spectra of Na/Ne have not been obtained. Second, symmetric splitting of the M $J = {}^3/_2$ energy level is not supported by Na/Ar spectra, and last, the 12-nearest-neighbor "supermolecule" is very difficult to justify in light of the multiple $^2S \rightarrow {}^2P$ absorption triplets[26−29] and the various relative sizes of the different alkali metal/rare gas combinations.

Most theoretical approaches to the MA question concerning the M/Rg systems start out from a symmetry basis: i.e., the site has this symmetry, so the system will behave this way. This site symmetry assumption will hold for F-centers, or other systems in which the impurity fits comfortably into a single substitutional or interstitial site in a crystal. It may also be useful for studying atoms in molecules, where the surroundings form a specific and guaranteed point group. Site symmetry is not such a good basis for analysis in cases such as the M/Rg systems where the M atom is likely contained in a cavity larger than a one Rg-atom vacancy. Under these conditions, identifying the site symmetry, assuming that it is consistent and symmetric, is not so easy. Furthermore, it is unlikely that even these assumptions will hold in all cases.

Because site symmetry cannot be guaranteed in many systems, including most M/Rg systems, the question of whether the site must be symmetric for MA to be valid becomes significant. It seems, on the basis of careful reading of the original moment analysis papers,[9,36] the papers on the physical basis for the model,[37,38] and our experience with the simulations, that the answer to this question is NO.

In fact, our simulations, described below, have consistently and conclusively demonstrated that site symmetry does not play a significant role in the MA derived spin−orbit results. The importance of this lack of variation with trapping site symmetry in the MA spin−orbit and g-factor results is that it shows there is no reason for any assumption of site symmetry in evaluating a system using the MA.

4. Monte Carlo Simulation of the Absorption and MCD Spectra of M/Rg

The simulation process utilized in modeling the $^2S \rightarrow {}^2P$ transition in a M/Rg system uses a classical Monte Carlo (MC) scheme based upon the original Metropolis et al. algorithm[39] exactly as implemented by Boatz and Fajardo for the case of electronic absorption spectroscopy[40] with extension to include MCD spectroscopy accomplished by Kenney et al.[5] A MC-MCD simulation begins by choosing an initial M−Rg configuration $\{M, R_1, R_2, ..., R_N\}_{initial}$, typically, representing an idealized trapping site [e.g., M in a single substitutional site (one-atom vacancy) with O_h symmetry]. The full MCD spectrum for a $^2S \rightarrow {}^2P$ transition in a M/Rg system in a specific M−Rg configuration $\{M, R_1, R_2, ..., R_N\}$ is a "stick MCD spectrum" consisting of 12 lines, appropriately placed on the x (energy) axis at transition energies $h\nu_{fi}$, whose magnitudes and directions (+ or −) on the y ($\Delta A'$) axis are determined by computing eq 2.5 as restated here,

$$\Delta A'(\nu_{fi}) = A'_{LCP}(\nu_{fi}) - A'_{RCP}(\nu_{fi}) \qquad (2.5')$$

for all possible choices of i and f and the prime indicates the measurement is taken in a magnetic field. To simulate a real MCD spectrum, many stick MCD spectra, each arising from a different Rg configuration, are appropriately averaged together. The MC energy optimization scheme operates in the ^2S ground-state manifold. At this stage, the very small Zeeman perturbation of the ^2S manifold is neglected. MCD stick spectra arising from more favorable configurations are weighted more heavily in the averaging process than those arising from the less favorable configurations. In actual practice, the LCP and RCP contributions to the MCD spectrum appearing in eq 2.5 are accumulated and stored separately. This allows the electronic absorption spectrum to be recovered from the MC-MCD simulation as[7]

$$A' = A = \frac{1}{2}[A'_{LCP} + A'_{RCP}] \qquad (4.1)$$

Equation 4.1 expresses the fact, well established experimentally, that the electronic absorption spectra of M/Rg systems are essentially unaffected by the application of an external magnetic field.

4.1. Orientational Averaging in MC-MCD Simulations. In an MCD experiment, the propagation direction of the light, which is always parallel to the **B** vector, rigorously defines the laboratory frame z axis. The laboratory frame x and y axes are set parallel to the sapphire deposition window and perpendicular to **B** with the origin at the M nucleus. All Rg positions, eigenvectors, and selection rules are described with respect to this laboratory frame. To model the effects of arbitrary Rg lattice orientation relative to the laboratory frame, the ^2P interaction matrix[5] is separated into M/Rg and spin−orbit + Zeeman matrices

$$[M/Rg + SO + Zeeman] = [M/Rg] + [SO + Zeeman] \qquad (4.2)$$

Arbitrary orientations of the Rg matrix relative to the laboratory frame can be modeled by rewriting eq 4.2 as

$$[M/Rg + SO + Zeeman] = [U][M/Rg][U]^{-1} + [SO + Zeeman] \qquad (4.3)$$

where U is an arbitrary randomly generated unitary rotation

matrix (e.g., a Eulerian rotation matrix). The MC-MCD simulation process is carried out as before using eq 4.3 rather than eq 4.2.

4.2. Lattice Temperature vs Magnetic Temperature in MC-MCD Simulations. Temperature effects appear in two distinct places in MC-MCD simulations. A lattice temperature, T, must be specified for the MC simulation process. It may be argued that a proper representation of quantum mechanical zero point vibrational motions of the M/Rg lattice at temperature T requires the classical MC simulation to be carried out at a classical lattice temperature $T' > T$.[41] However, a temperature for the Boltzmann factor of the Zeeman-split ^{2}S term also must be included. This "magnetic temperature" always should be the actual system temperature, T. The MC-MCD simulation code has the option of specifying separate values for the lattice temperature T' and the magnetic temperature T_{mag}. Lawrence and Apkarian discuss the relationship between T' and T_{mag} in classical MC simulations of doped Rg systems.[41]

4.3. Truth-Testing of MC-MCD Simulations. At this point it should be noted that the MC-MCD simulation code based upon the theory outlined in ref 5 and used with this work has passed the following tests in Na/Ar. The MC-MCD spectra (and associated absorption spectra) (1) exhibit MCD and absorption band profiles that look very similar to the experimental spectra of M/Rg systems, (2) properly overlay each other in energy, (3) properly invert when the direction of the magnetic field is reversed, (4) increase or decrease in amplitude with increases or decreases in B, (5) yield proper spin−orbit coupling constant magnitudes and signs from band moment[7] analyses, and (6) are suitably responsive to temperature effects and orientational averaging.

5. Evaluation of the Simulations Using the MA Method

A computer program was written to calculate the moment integrals on the simulated spectra produced by the MC-MCD program. Because the ^{2}P SO coupling constant sign and magnitude, trapping site symmetry, magnetic field, and temperature(s) can be chosen explicitly in the simulation, a successful MA method must recover these parameters from the simulated $^2S \rightarrow {}^2P$ absorption and MCD spectra that are calculated to arise from this simulated M/Rg system. Therefore, if the MA method did not produce the expected spin−orbit splitting, it would be precisely falsified for the M/Rg systems. The MA consistently reproduced the input spin−orbit splitting to within reasonable variations. As yet, the only times in which the MA has not reproduced the input SO splitting within the error bounds is when the input magnetic field is large. In the cases examined, as the magnetic field is increased, the MA increasingly underestimates the SO splitting. This is not, however, a major concern, because most experimental MCD spectra are acquired with magnetic fields much smaller than those produced by these deviations in the simulations.

In this study, a MA data set is constructed by generating a set of simulated absorption and MCD spectra using multiple magnetic temperatures; typically, $T_{mag} = 4$, 6, 8, 10, 20, and 30 K, are used. A single substitutional site was used in generating all of the simulated absorption and MCD spectra. The moment integrals, eqs 3 and 4, are evaluated numerically using Simpson's rule. For each temperature, the first, second, and third MCD moments and the zeroth and second absorption moments are calculated. The ξ^2 term used in calculating the cubic and noncubic vibronic mode parameters, Δ_C^2 and Δ_{NC}^2, is derived from the slope of the spectral data, though it can also be calculated directly from ξ. Then g, ξ, Δ_C^2 and Δ_{NC}^2 are calculated from eqs 3.1, 3.2, 3.3, and 3.4. The technique was tested by tabulating spectra from the literature and comparing the results with those published. The SO splittings obtained from the MA generally were in good agreement with the values input into the simulations, with deviations accounted for by the numerical errors associated with tabulating the spectra and calculating the moment integrals.

Single spectrum MA of simulation or experimental data is also possible. This requires that an assumption for the g-factor be made for the initial calculation. For simulation data a g-factor of 1, the average of the atomic P-state g-factors, is a good approximation. This is because unaltered simulation spectra consistently produce $g \approx 1.00$ in the MA evaluation.

For experimental data, the choice of g is not so clear, because it is conceivable that the true value may differ from the atomic average. In fact, Adrian[42] claims that the matrix g-value is necessarily smaller than the free atom g-value due to mixing of the matrix atom properties into the isolated atom wave function. This overlap causes the matrix SO interaction to have the effect of reducing the g-value, regardless of the nature of the trapping site, although the difference is $\sim 10^{-4}$ or less for a trapped hydrogen (H) atom.[42] Reductions in the magnitude of the g-value were also calculated by Smith [in ref 43, p 25] for the alkali atoms trapped in solid rare gases.

Therefore, when the experimental spectrum tested is from published sources, the published g-value may be used. If no g-factor is available, or its accuracy may be in doubt, an estimate of the g-factor can usually be obtained from the ratios of M_1/A_0 and M_2/A_0. M_2/A_0 gives an estimate of ξ^2, from which the positive and negative roots may be substituted into eq 3.1, producing two possible g-values. Generally, one of these can be rejected, identifying the correct root of ξ^2 and therefore the best estimate of the SO splitting, ξ. This technique for estimating g fails when $(M_2/A_0) < 0$. This unphysical situation has often occurred in simulation results. It is not known if it may also happen with experimental results, though some researchers have not used this value in analyzing their data because it is unreliable.[1]

Because the single spectrum MA technique described here rests, to a certain extent, on the choice of g-factor, it seemed prudent to test the sensitivity of the calculation to it. It was found that the g-factor has no effect on the cubic mode parameter, Δ_C^2, and only limited effect, through the value of ξ^2 used, on the noncubic mode parameter, Δ_{NC}^2. The same cannot be said of the SO splitting. Our simulation tests indicate that the choice of g-value affects the MA calculated SO splitting in a consistent pattern, with the calculated SO splitting increasing with increasing g-value. For systems having large SO splittings, the variation in the SO splitting with g-value is significant, but not extreme. When the SO splitting is small, however, these variations can be greater than the total SO splitting.

In this test, the g-value used to calculate the SO splitting was varied from 0.0 to 2.0 in steps of 0.5. In each case, the calculated SO splitting was reduced by ~ 20 cm^{-1} for $g = 0.0$, and increased by ~ 20 cm $^{-1}$ for $g = 2.0$ compared to the value calculated for $g = 1.0$, the free atom value. The trapping site was a one-atom vacancy, the magnetic field, $B = 1$ T, and the selected magnetic temperature, $T_{mag} = 10$ K. Table 2 displays the results of this test. The spin−orbit splittings between the double line are the input values used in generating the simulated spectra. The values listed across from the g-values are those calculated using that g-value and the ratio M_1/A_0.

TABLE 2: Effect of the *g*-Value on the Single Spectrum MA Calculated SO Coupling

	calculated SO splitting		
g	−170.0 cm^{-1}	170.0 cm^{-1}	17.0 cm^{-1}
0.0	−190.7	149.1	−3.9
0.5	−180.3	159.6	6.5
1.0	−169.9	170.0	16.9
1.5	−159.4	180.4	27.4
2.0	−149.0	190.8	37.8

6. Exploration of Governing Factors in MA Results

6.1. Spin−Orbit Splitting and the MA Method. In general, the absorption spectra for all simulation tested spin−orbit coupling values are very similar. In fact, when the SO splitting is in the range ±50 cm^{-1}, the same trapping site at the same temperature produces identical absorption spectra down to expected statistical errors inherent in Monte Carlo (MC) sampling. The exceptions tested, ±170 cm^{-1}, have SO splittings on the same order of magnitude as the M−Rg and Rg−Rg matrix interaction energies. The diatomic interaction potentials show that the argon−argon binding energy is around 100 cm^{-1}, and the sodium−argon (Na−Ar) binding energy is around 58 cm^{-1}.

This suggests that the MA results depend primarily on the MCD spectral features. To explore this theory, several tests were instituted. In the first test, two sample data sets were constructed. One of these had the absorption spectrum generated with input SO splitting at −170 cm^{-1} and the MCD spectrum generated with SO splitting of 17 cm^{-1}; the second had the reverse with the absorption SO splitting = 17 cm^{-1} and MCD SO splitting = −170 cm^{-1}. These input SO splitting values were chosen because both produce an MCD spectrum characterized by two down peaks and one up peak with increasing energy. This test strongly supported the preeminence of the MCD spectrum in determining the MA SO splitting. For the set with the MCD generated using an input SO splitting of 17 cm^{-1} the MA calculated SO splitting was 16.87 cm^{-1}, easily in the range of expected MA SO splitting values for a simulation set with input SO splitting of 17 cm^{-1}. In the reverse test where the MCD SO splitting was −170 cm^{-1}, the MA calculated SO splitting was −263.43 cm^{-1}. The reason for the substantial increase in the magnitude of the SO splitting in this case is not entirely understood but is probably a function of the relatively large contribution of the outer edges of the MCD spectra in comparison to the absorption, as supported by the tests of the spectral bandwidth reported later in this paper. Typically, the relative intensity of the MCD spectrum is several orders of magnitude less than the absorption spectrum over the entire spectral range. In this case, however, the MCD band was broader than the absorption band; consequently, it has a significant intensity where the absorption is small. This could occur experimentally if the zero point of the absorption is incorrectly defined or absorption is present, but not significant compared to the maximum of the spectra. The simulations have shown that $\Delta A'/A$ is larger for larger magnitude SO splittings than for smaller magnitude SO splittings. Therefore if $\Delta A'/A$ is artificially inflated, the result is a larger magnitude calculated SO splitting, with the peak pattern determining a negative sign for the SO splitting. The magnitude of $\Delta A'/A$ also plays a role in whether the MCD peak pattern of down, down, up is calculated as a positive SO coupling or negative SO coupling. Smaller $\Delta A'/A$ tend to produce positive SO splitting values for this pattern.[32]

To further explore the effect of the MCD on the MA calculated SO results, a second test in which the MCD of a specific set is multiplied by a scale factor was conducted. In this test the resultant MA calculated SO splitting was consistently equal to the value of the input SO splitting multiplied by the scale factor. Similarly, the calculated *g*-factor varied directly with the scale factor. When no scaling occurred, the MA calculated SO splitting is approximately equal to the input SO splitting, and the *g*-factor is approximately equal to the averaged atomic M P-state value of 1. Although it may be very difficult to experimentally verify, this suggests that faulty MA results can occur if something other than the SO splitting is a major factor in producing the relative heights of the MCD and absorption bands. It further suggests that the *g*-factor might provide an estimate of the degree of error in the SO splitting measurement. Table 3 demonstrates the variation in the MA calculated SO splitting and calculated *g*-factor when the MCD spectra for a 1-atom vacancy with input SO splitting of 17 cm^{-1} are scaled by multiplying the MCD intensity by a selected scale factor. Included in the table for comparison are the input and MA calculated SO splittings, and the MA calculated *g*-factors. Notice that the *g*-factors for the unscaled sets (column 6, Table 3) are all approximately 1. Table 4 is the corresponding table for input SO coupling of −170 cm^{-1}. The values here can be compared with those in Table 3.

TABLE 3: Effect of Scale Factor on Spectra

	from scaled[a]		from original		
scale factor	calc SO (cm^{-1})	*g*-factor	input SO (cm^{-1})	calc SO (cm^{-1})	*g*-factor
1.0	16.87	1.00	17		
−1.0	−16.87	−1.00	−17	−16.89	1.00
10.0	168.72	9.97	170	167.74	0.96
−10.0	−168.72	−9.97	−170	−169.02	1.07
5.0	84.36	4.99		N/A	N/A
−5.0	−84.36	−4.99		N/A	N/A
3.0	50.61	2.99	50	49.66	0.99
−3.0	−50.61	−2.99	−50	−49.68	1.00
0.6	10.12	0.60	10	9.94	1.00
−0.6	−10.12	−0.60		N/A	N/A

[a] Initial SO splitting = 17 cm^{-1}.

TABLE 4: Effect of Scale Factor on Spectra[a]

	from scaled	
scale factor	calc SO (cm^{-1})	*g*-factor
0.1	−16.80	0.10
−0.1	16.80	−0.10
0.3	−50.40	0.31
−0.3	50.40	−0.31
1.0	−168.00	1.03
−1.0	168.00	−1.03

[a] Initial SO splitting = −170 cm^{-1}.

The possibility that some factor might influence the width of the MCD bands with respect to the absorption bands was also considered. The spectral bandwidths of the simulated absorption and MCD spectra were separately broadened or narrowed by adjusting energy steps (aka nominal simulation bin size) in the calculation of the moment integrals. In some cases, the energy barycenter of the absorption or MCD was shifted with respect to the original placement. It was found that broadening or narrowing the absorption spectra has very little effect on the SO splitting results (see Table 5.) However, the same is not true of changes in the MCD bandwidth. These had a proportionate effect on the MA calculated SO splitting. Broadening or narrowing either the absorption or MCD spectrum, but not the other, in all cases significantly affected the cubic and noncubic vibronic mode parameters, sometimes making one or more of the M_2/A_0 ratios less than zero, an

TABLE 5: Effects of Spectral Bandwidth on MA Results[a]

		Landé *g*-factor calcd from:			squares of (vibronic)	
test	SO coupling (from slope) (cm^{-1})	slope	M_2/A_0	input SO (cm^{-1})	cubic mode param (Δ_C^2)	noncubic mode param (Δ_{NC}^2)
1	16.87	0.997	0.999	1.005	395.525	71991.039
2	18.56	1.097	NAN	1.007	22297.029	43489.871
3	15.18	0.898	0.965	1.002	−21336.740	101785.312
4	16.87	0.997	1.038	1.005	−23627.068	120000.828
5	16.87	0.997	0.913	1.005	19888.279	32861.023
6	20.26	1.197	NAN	1.009	44570.574	15713.099
7	13.49	0.798	0.863	1.001	−43943.586	134465.422
8*	15.08	0.892	NAN	1.003	−20047.752	100496.984
9*	15.18	0.898	0.899	1.003	345.754	58283.531
10*	16.98	1.003	NAN	1.004	30884.021	21864.361
11	16.86	0.997	1.059	1.005	−52429.555	177575.953
12	25.31	1.496	1.495	1.014	561.952	162361.500
13	25.25	1.493	NAN	1.015	112872.141	−64713.969
14*	17.73	1.052	NAN	1.010	295392.812	−229599.203
15*	19.96	1.174	NAN	1.002	793403.500	−727628.562

[a] Tests marked with an asterisk have the MCD or absorption energy center shifted with respect to the original placement. The Landé *g*-factor calculated from M_2/A_0 is "NAN" (not a number) when M_2/A_0 is less than zero for at least one simulation in the data set.

TABLE 6: Spectra Broadening Test Parameters[a]

	MCD		absorption	
test	energy bin size (cm^{-1})	starting energy (cm^{-1})	energy bin size (cm^{-1})	starting energy (cm^{-1})
1	10	13990	10	13990
2	11	13594	10	13990
3	9	14386	10	13990
4	10	13990	11	13594
5	10	13990	9	14386
6	12	13198	10	13990
7	8	14782	10	13990
8	9	14440	10	13990
9*	9	14440	9	14440
10	10	13990	9	14440
11	10	13990	12	13198
12*	15	12040	15	12040
13	15	12040	10	13990
14	11	13990	10	13990
15	11	12980	10	13990

[a] Tests marked with asterisk used the same bin size for the absorption and MCD.

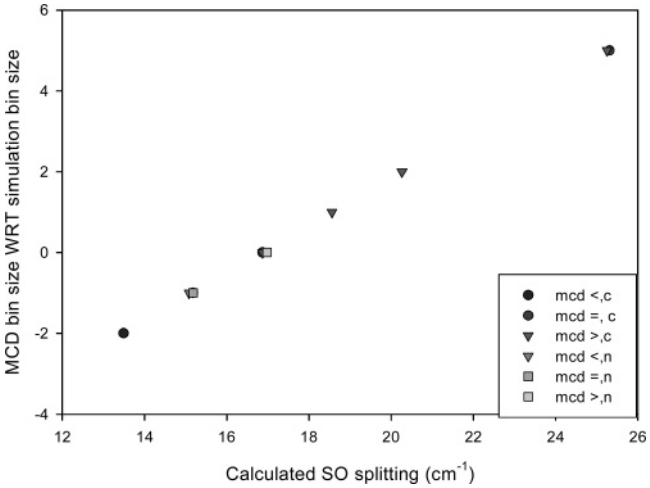

Figure 1. Effect of adjusting the MCD bin size on the calculated spin−orbit splitting parameter. <, >, and = in the legend means the MCD bin size is set smaller than, larger than, or equal to, respectively, the corresponding absorption bin size; c means the MCD bins are centered on the true simulation absorption barycenter, and n means they are not.

unphysical result. Broadening or narrowing both the absorption and MCD spectra tended to keep these values more stable. Table 6 gives the energy bin sizes and starting energies for the MCD and absorption spectra. The unaltered (default) bin size is 10 cm^{-1}.

Figure 1 shows the effect of varying the MCD bin size, plotting the SO splitting from Table 5, against the variation of the MCD bin size with respect to the simulation bin size. Although there are minor variations in the calculated SO splitting depending on the difference between the entered values for the MCD and absorption bin sizes or whether the starting value of the MCD and absorption energies have been adjusted to keep the energy barycenter in its original position, it is safe to say that the MCD bin size is the dominant factor in the calculated SO splitting.

Interestingly, small displacements of the MCD with respect to the absorption do not have a significant effect on the MA calculated SO splitting. Sample data files were created by shifting the MCD and absorption spectrum energy axes with respect to one another by a small interval δ_E; then MA was performed on a data set. The unshifted data set had a MA calculated SO coupling of 16.87 cm^{-1}. Shifting the MCD relative to the absorption 100 cm^{-1} made the MA calculated SO coupling 17.05 and 16.68 cm^{-1}, when the MCD was shifted to a lower energy or a higher energy, respectively, compared to the absorption. Considering the magnitude of the total relative shift between the MCD and absorption, these changes in the calculated SO splitting are negligible.

Non-spin−orbit sources that may contribute to the MCD spectra include the pseudo-Jahn−Teller-effect (PJTE) and orbit lattice coupling. The PJTE is the vibrational mixing of "the finite electronic state with another closely located electronic level",[44] which can influence the energies and spacing of the levels. Orbit−lattice couplings, coupling of the electron orbit to lattice vibrations, may sizably change the energy spacings of the levels.[45] It has also been suggested that external axial crystal fields can mimic SO coupling.[46]

The basic conclusion that can be drawn from the tests of the MA governing factors is that though the MA method is relatively impervious to any changes to the absorption spectra, the same cannot be said of variations in the MCD spectra. Depending on the source of variation, the effects of modifications to the MCD spectra can range from negligible to substantial.

6.2. Jahn−Teller Vibronic Mode Parameters, Δ_C^2 and Δ_{NC}^2. Although the MA has been extremely successful in

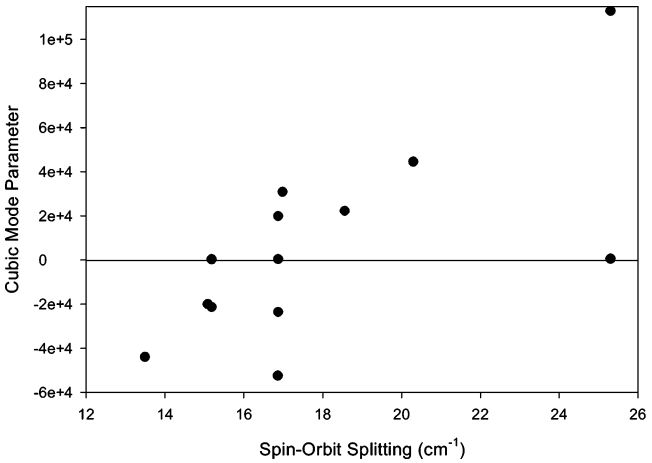

Figure 2. Plot of the square of the cubic mode parameter verses spin−orbit splitting from Table 5, except two (see text). All values below the horizontal line are unphysical because because the parameter being represented is a square and cannot therefore be negative.

extracting the spin−orbit splitting of the simulations, and hence the *g*-factor, the results for the square of the cubic vibronic mode parameter and, to a lesser extent, the square of the noncubic vibronic mode parameter, have been highly erratic. Dramatic changes in the value of the square of the cubic mode parameter occur with simple changes in the choices of magnetic temperatures evaluated in a single set of simulations. In some cases, this value has been negative, which is not physically possible, because it is a squared parameter. Because these parameters are vibronic in nature, and specifically apply to symmetric sites, their inclusion in MA of M/Rg systems, with the possible exception of Li/Xe, are suspect. They are a holdover from the f-center origins of the MA equations. Consequently, their applicability to the M/Rg systems was not questioned or tested. Although the failure of vibronic modes, Δ_C^2 and Δ_{NC}^2, in simulation results is not proof that the values are not valid in experimental results, it certainly casts doubt on their applicability. Furthermore, dynamic Jahn−Teller (DJT) analysis of Li/Xe results[47] also cast doubt on the validity of the MA derived values of the vibronic modes, Δ_C^2 and Δ_{NC}^2. In this study, a Jahn−Teller analysis, assuming an octahedral, O_h, trapping site and equal coupling of the t_{2g} and e_g vibrations, was able to replicate the observed absorption and MCD spectra with reasonable success. However, the values of Δ_C^2 and Δ_{NC}^2 entered into the JT analysis producing these results were NOT the values obtained through the MA. Rather the parameters were adjusted until the best fit to the data was obtained. Furthermore, the theory is insufficient to account for other alkali atom spectra.[47]

Figure 2 is a graphical representation of the scatter in the cubic mode parameter as it varied with the method test shown in Table 5. The values from tests 14 and 15 were excluded from this table as they were so large that they made the range scale unreasonable. Although there is an apparent trend to higher values of the cubic mode parameter with increasing apparent SO splitting, this cannot be assumed to be the case; by focusing only on the values right around 17 cm^{-1}, it can be seen that the distribution is very random. Negative values of the cubic mode parameter are not possible because it is a squared value; therefore all values below the blue line represent unphysical results. The noncubic mode parameter is not plotted but typically scales inversely with the cubic mode parameter, going negative (again an unphysical result) when the cubic mode parameter is very large. In all of these cases, the same trapping site, a single substitutional site (aka one-atom vacancy), was used.

The Jahn−Teller effect is defined to be the vibronic lifting of electronic degeneracy in symmetric trapping sites. If the trapping site is inherently asymmetric, then this degeneracy may be partially or wholly lifted by crystal field effects. Furthermore, using MA to get Jahn−Teller strengths from an asymmetric site may have the effect of artificially inflating the MA calculated values of the vibronic modes. In the simulations, the magnitudes of the vibronic modes, Δ_C^2 and Δ_{NC}^2, are consistently larger in the asymmetric sites than in the symmetric sites. Typically, the squares of the asymmetric site cubic mode parameters were 2 orders of magnitude larger, whereas the squares of the noncubic mode parameters were an order of magnitude larger than those for the symmetric sites. This is a significant difference, and overlooking this possibility may lead to substantial errors in analysis of a system.

The only possible exception to the lack of site symmetry influence occurs in the higher order moments in the MA analysis. The ratios of some of these are purported to provide information on the vibronic modes in the system, as well as a second check on the magnitude of the spin−orbit splitting. This information has been used to draw conclusions about the strength of the Jahn−Teller active modes in the system. There are a couple of problems with this usage. First, these values tend to be highly random, and second, for most M/Rg systems, the trapping sites cannot be assumed to be symmetric. If the sites are asymmetric, the JTE cannot operate, so the physical significance of the higher order moments is called into question.

7. Conclusion

When we initially considered the experimental results derived from the MA method, we concluded that they could not possibly be right. This conclusion was based on both the explanations provided for the results and the trapping site symmetry assumptions used in connection with the MA equations. The theoretical evaluations of the results either were not consistent with the experimental results or were based on faulty physics. The symmetry assumptions for the trapping sites simply were not consistent with multiple trapping sites in a single rare gas nor were they consistent with the relative sizes of the different metals/rare gas host atoms. However, MA of simulated spectra consistently returned the input SO splitting, providing an independent confirmation of the MA method for this value in the M/Rg systems. Further investigation into the MA method showed that the symmetry assumptions were based on f-center trapping sites and are not necessary to MA in general. Therefore, the simulations and subsequent study have shown that the MA method is valid for M/Rg systems; however, the equations containing the JT vibrational information should not be used.

It is possible that the lack of significant variation in the MA generated SO splitting with trapping site is not entirely accurate. Any configuration-dependent influences on the SO splitting are not well determined and therefore not explicitly included in the physical basis for the simulations. The importance of the site symmetry is more accurately ascribed to the SO splitting that will exist in the real system, because it will play a role in the electron−lattice interaction, which in turn affects the SO splitting of the atom or molecule.

Several tests of the spectral features that can influence the spectra and therefore the MA results were conducted. These demonstrate the sensitivity of the MA method to variations in the MCD spectra, highlighting the need for extra care when measuring MCD spectra. Further simulation tests of the factors influencing MA results for M/Rg systems will be presented in future papers.

References and Notes

(1) Lund, P. A.; Smith, D.; Jacobs, S. M.; Schatz, P. N. *J. Phys. Chem.* **1984**, *88*, 31−42.

(2) Rose, J.; Smith, D.; Williamson, B. E.; Schatz, P. N.; O'Brien, M. C. M. *J. Phys. Chem.* **1986**, *90*, 2608−2615.

(3) Hormes, J.; Schiller, J. *Chem. Phys*. **1983**, *74*, 433−439.

(4) Rose, J. L. Matrix-isolation studies of alkali metal, free radicals and the components of the organic molecule TTF-TCNQ. Ph.D. Thesis, University of Virginia, 1987.

(5) Kenney, J. W., III; Boatz, J. A.; Terrill Vosbein, H. A. *Int. J. Quantum Chem*. **2005**, *103*, 854−865.

(6) Kruglov, V. P.; Gribov, L. A. Automation of determination of parameters of spectral bands with a computer. *Bull. Timiryazev Agric. Acad.* **1972**, *1*, 212−219. Translated from the original Russian by Nikolay Lepeshkin.

(7) Piepho, S. B.; Schatz, P. N. *Group Theory in Spectroscopy with applications to Magnetic Circular Dichroism*; Wiley: New York, 1983.

(8) Kruglov, V. P.; Gribov, L. A.; Chekunov, A. V. Numerical determination of the moments of spectral band with the computer "MINSK-22". *Izv. Timiryazevsk. Skh. Akad. (Bull. Timirjazev Agric. Acad.)* **1972**, *4*, 17−181. Translated from the original Russian by Nikolay Lepeshkin.

(9) Henry, C. H.; Snatterly, S. E.; Schlickter, C. P. *Phys. Rev*. **1965**, *137*, A583.

(10) Stephens, P. J. Magnetic circular dichroism. *Adv. Chem. Phys.* **1976**, *35*, 197−264.

(11) Zgierski, M. Z. *J. Chem. Phys.* **1985**, *83*, 2170−2185.

(12) Zgierski, M. Z. *Chem. Phys. Lett.* **1985**, *118*, 547−552.

(13) Samet, C.; Rose, J. L.; Williamson, B. E.; Schatz, P. N. *Chem. Phys. Lett*. **1987**, *142*, 557−561.

(14) Samet, C.; Rose, J. L.; Schatz, P. N.; O'Brien, M. C. M. *Chem. Phys. Lett*. **1989**, *159*, 567−572.

(15) Gorller-Walrand, C.; et al. *J. Chem. Phys*. **1985**, *82*, 1212−1230.

(16) Miller, J. C.; Mowery, R. L.; Krausz, E. R.; Jacobs, S. M.; Kim, H. W.; Schatz, P. N.; Andrews, L. *J. Chem. Phys.* **1981**, *74*, 6349−6361.

(17) Graham, R. G.; Grinter, R. *J. Chem. Phys*. **1989**, *91*, 6677−6683.

(18) Singer, R. J.; Grinter, R. *Chem. Phys*. **1987**, *113*, 99−109.

(19) Singer, R. J.; Grinter, R. *Chem. Phys.* **1987**, *117*, 449−456.

(20) Vala, M.; Zeringue, K.; Shakhs-Emampour, J.; Rivoal, J.-C.; Pyzalski, R. *J. Chem. Phys*. **1984**, *80*, 2401−2406.

(21) Vala, M.; Ering, M.; Pyka, J.; Rivoal, J.-C.; Grisolia, C. *J. Chem. Phys.* **1985**, *83*, 969−974.

(22) Grinter, R.; Stern, D. R. *J. Mol. Struct*. **1982**, *80*, 147−150.

(23) Rivoal, J.-C.; Vala, M. *J. Chem. Phys*. **1987**, *86*, 5958−5962.

(24) Zeringue, K. J.; ShakhsEmampour, J.; Rivoal, J.-C.; Vala, M. *J. Chem. Phys*. **1983**, *78*, 2231−2239.

(25) Hormes, J.; Grinter, R.; Breithaupt, B.; Kolb, D. M. *J. Chem. Phys.* **1983**, *78*, 158−166.

(26) Fajardo, M. E.; Carrick, P. G.; Kenney, J. W. *J. Chem. Phys*. **1991**, *94*, 5812−5825.

(27) Fajardo, M. E. *J. Chem. Phys*. **1993**, *98*, 110−118.

(28) Tam, S.; Fajardo, M. *J. Chem. Phys*. **1993**, *99*, 854−860.

(29) Corbin, R.; Fajardo, M. *J. Chem. Phys*. **1994**, *101*, 2678−2683.

(30) Stowe, S. L. Magnetic circular dichroism spectroscopy of alkali metal atoms trapped in cryogenic noble gas matrices. Master's thesis, Eastern New Mexico University, 1993.

(31) Kenney, J. W., III. Magnetic circular dichroism (MCD) spectroscopy of cryogenic metal containing matrices prepared by laser ablation. HEDM Contract No. F29601-91-C-0015, AFOSR, 1994.

(32) Terrill, H. A. *Exploring the Theory of the Magnetic Circular Dichroism and Electronic Absorption Spectra of Alkali Metals Matrix Isolated in Rare Gas Solids, II*. Ph.D. Thesis, New Mexico State University, 1999.

(33) Ham, F. S. *Phys. Rev*. **1965**, *138*, A1727−A1740.

(34) Pellow, R.; Vala, M. *J. Chem. Phys*. **1989**, *90*, 5612−5621.

(35) Strek, W.; Wierzchaczewski, M. *Acta Phys. Polon.* **1981**, *A60*, 857−865.

(36) Henry, C. H.; Slichter, C. P. Moments and degeneracy in optical spectra. In *Physics of Color Centers*; Beall Fowler, W., Ed.; Academic Press: New York, 1968; Chapter 6, pp 351−428.

(37) Van Vleck, J. H. The dipolar broadening of magnetic resonance lines in crystals. *Phys. Rev.* **1948**, *74*, 1168−1183.

(38) Van Vleck, J. H. *The Theory of Electric and Magnetic Susceptibilities*; Oxford University Press: London, 1959.

(39) Metropolis, N.; Rosenbluth, A. W.; Rosenbluth, M. N.; Teller, A. H.; Teller, E. *J. Chem. Phys*. **1953**, *21*, 1087.

(40) Boatz, J.; Fajardo, M. *J. Chem. Phys.* **1994**, *101*, 3472−3487.

(41) Lawrence, W. G.; Apkarian, V. A. *J. Chem. Phys.* **1994**, *101*, 1820−1831.

(42) Adrian, F. J. *J. Chem. Phys*. **1960**, *32*, 972−981.

(43) Weltner, W., Jr. *Magnetic Atoms and Molecules*; Scientific and Academic Editions: New York, 1983.

(44) Perlin, Y. U E.; Kharchenko, L. S.; Gyndya, L. G. Psuedo-Jahn−Teller effect in tetragonal local centers. Translated from *Izv. Vyssh. Uchebn. Zaved., Fiz.* **1987**, *12*, 62−67.

(45) Varret, F.; Ducouret-Cereze, A. *J. Physique* **1988**, *49*, C8-847−C8-848.

(46) Pustovit, A. V.; Yu. Shulepov, V.; Ksenofontov, V. G. Translated from *Teor. Eksp. Khim.* **1989**, *25*, 308−311 (333−336).

(47) O'Brien, M. C. M. *J. Phys. C: Solid State Phys.* **1985**, *18*, 4963−4973.